



Experimental Investigation on Humidity Sensing of Nanostructured Ferric Oxides

Richa Srivastava^{1,2,*}, Satyendra Singh², Nidhi Verma²

¹Department of Engineering Physics, UIET, Babasaheb Bhimrao Ambedkar University, Lucknow, India

²Nanomaterials and Sensors Research Laboratory, Department of Physics, University of Lucknow, Lucknow, India

Email address:

richadolly@rediffmail.com (R. Srivastava), satyendra_nano84@rediffmail.com (S. Singh), nidhi_gsensor10@rediffmail.com (N. Verma)

*Corresponding author

To cite this article:

Richa Srivastava, Satyendra Singh, Nidhi Verma, Experimental Investigation on Humidity Sensing of Nanostructured Ferric Oxides.

Advances in Nanomaterials. Vol. 1, No. 1, 2017, pp. 16-21. doi: 10.11648/j.an.20170101.14

Received: March 7, 2017; **Accepted:** April 20, 2017; **Published:** June 22, 2017

Abstract: Nanostructured ferric oxides (A and B) were synthesized via chemical precipitation method using two different precipitating agents i.e. ammonium hydroxide and sodium hydroxide. X-ray diffraction proved the formation of ferric oxide. Crystallite sizes of the materials A and B were 40 and 18 nm respectively. Surface morphology of sample B reveals that it has more adsorption sites in comparison to A. Further the pellets and thick films of materials A and B were prepared and investigated with the exposition of humidity from 10%RH to 90 %RH. It was found that the thick film prepared with material B was most sensitive among all having maximum average sensitivity 8.12 MΩ/%RH. Good sensitivity, less hysteresis, and reproducibility identify that fabricated humidity sensor (B) is promising for the device application.

Keywords: Humidity Sensor, Surface Morphology, Sensitivity, Nanomaterials

1. Introduction

Effects of humidity on various materials are well known for a long time in many ways. It affects mankind directly or indirectly. The irreversible effect due to humidity eventually causes permanent damage to the exposed surfaces. Therefore, there is an urgent need to measure and control precisely the humidity in various environments [1]. Ferric oxide has a wide range of applications as magnetic material [2-8], but in recent years many researchers investigated Fe₂O₃ as humidity sensitive material [9-12]. It is considered to be the most promising highly sensing materials for sensors due to the temperature dependent surface morphology and stability [13].

Surface morphology plays an important role for enhancing the sensitivity and stability of the fabricated sensor [14-18]. Regarding this point of view, ferric oxide is challenging material for fabrication of humidity sensor. In many parts of the world, researchers have been trying to fabricate humidity sensor having most sensitivity, stability, low hysteresis, quick response and short recovery times. Synthesis and functionalism of nanostructured ferric oxide have attracted great interest due to their significant potential applications

[19-23]. Consequently, ferric oxide nanostructures, such as nanowires, nanobelts, nanoflowers and other special nanostructures have been successfully synthesized using various approaches [24-28]. In applications for humidity sensor devices, lower density and higher surface area are required. With this intention, several methods of preparation of ferric oxides are known. Co-precipitation, micro-emulsion, pulsed wire discharge and hydrothermal processes were employed worldwide in order to obtain nano-sized powder [29-30].

Present work reported the application part as humidity sensing of nanosized ferric oxide (A and B). Sample A and B were synthesized by hydroxide precipitation method using two different precipitation agents. The synthesized materials were characterized by Scanning electron microscope and X-ray diffractometer. Further, the solid state pellets and thick films were fabricated. The sensitivity of the film sensor was found better in comparison to the pellet sensor and is an advanced step towards the development of reliable humidity sensor. The sensitivity of the fabricated sensor (material B) was found better with respect to prior reported works [9, 31-33].

2. Synthesis of Materials

We have synthesized two samples of ferric oxide and the samples were named as A and B. For the synthesis of material A, ferric sulphate was precipitated by drop wise addition of ammonium hydroxide. The solution with the precipitate was thoroughly stirred for 2h in the ambient environment. After filtration, the precipitate was dried and annealed at 400°C for 2 h.

For the synthesis of the material B, sodium hydroxide was added drop by drop into 0.1 M ferric chloride solution with vigorous stirring for 6 h. The solution was cooled naturally to room temperature. The product thus obtained was washed successively with deionized water and then dried and annealed at 400°C in an electrical furnace for 2 h.

The synthesized powder A and B were compacted into pellets having thickness 3 mm and diameter 9 mm at a pressure of 618 MPa using a hydraulic press (M.B. Instruments, Delhi). Also, the thick films of samples A and B were prepared by screen printing method on two separate alumina substrates.

For the fabrication of the films, the synthesized powders were dissolved in isopropyl alcohol and these were sonicated for 15-20 min. The sonicated solutions were stirred at 80°C for 6 h. The obtained pastes were used for fabrication of thick films using screen printing technology. Took the paste of A and B and these paste were screen printed on to alumina substrate. The films were drying at 120°C for 4 h. This drying procedure stabilizes the films. Further, the films were annealed at 400°C which transforms the films as sensing materials. The silver contacts on two opposite ends of the films were made. Sensing films with silver contacts were used for humidity sensing measurements.

3. Characterizations of Materials

3.1. X-ray Diffraction (XRD) Analysis

The phase identification and crystallite size of the powdered material were analyzed using X-ray diffractometer (X-Pert, XRD system, Netherland) having $\text{CuK}\alpha$ radiations as a source with wavelength 1.5406Å. The XRD patterns of materials A and B show pure $\alpha\text{-Fe}_2\text{O}_3$ phase for sample A and B [34]. The average crystallite size was 40 nm for A. For B, the broadening of the XRD peaks arises primarily due to the fine particle size of the powder. The diffraction peaks of Bare much broadened compared to A sample, indicating the presence of very fine crystallite size. The average crystallite size for material B was 18 nm. Miller indices (h k l) for each diffracted peaks for A and Bare indicated on the diffraction pattern.

3.2. Scanning Electron Microscopy Analysis

The surface morphologies of the fabricated films were analyzed using scanning electron microscope (SEM, LEO-Cambridge and JEISS). The surface morphology of the films of materials A and B were investigated [34]. The film of

material B, shows more active sites, giving a largest effective surface area for adsorption of humidity which enhances the response of the sensor. The improved humidity sensing performance of B may be attributed to their porous spherical structure and crystallite size.

4. Measurements of Humidity Sensing Properties

Experimental set up for humidity sensing measurements is shown in Figure 1. In this arrangement, a saturated solution of potassium hydroxide was used as a dehumidifier and a saturated solution of potassium sulphate was used as a humidifier. The humidifier/dehumidifier was kept in a dish on a stand. Variations in %RH (relative humidity) were measured with the help of hygrometer (Huger, Germany) and variations in resistance were measured using Keithley electrometer (Model: 6514). The temperature of the chamber remained the same throughout the observations. The prepared pellets were put within a conductivity-measuring holder having Ag-pellet-Ag electrode arrangement. The silver contacts on two opposite ends of the films were made.

The prepared sensing thick films were put within the humidity chamber. Initially, the chamber was dehumidified up to 10% RH and the corresponding resistance of the sensing element was recorded. Later the humidification inside the chamber was carried upto 90% RH using a saturated solution of potassium sulphate and corresponding variations in electrical resistance were recorded. It was observed that as %RH inside the chamber increases from 10-90%RH, the resistance of the sensing material decreases over the entire range of RH.

The sensitivity of humidity sensor is defined as the change in resistance (ΔR) with per unit change in %RH as given in below:

$$S = \frac{\Delta R}{\Delta \%RH} M\Omega/\%RH$$

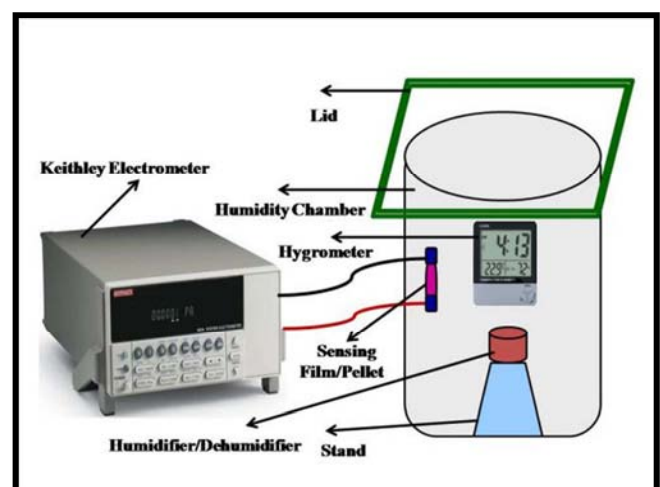


Figure 1. Experimental set up for humidity sensing measurements.

5. Results and Discussion

5.1. Study of Humidity Sensing Properties

Figure 2 (a) illustrates the variations in resistance with %RH for the pellet and film prepared using material A. The film prepared from A shows large variation of resistance and maximum average sensitivity 12.8 MΩ/%RH in lower humidity range 10-35% RH in comparison to pellet of A as shown in Figure 2(a). The average sensitivity for a film of A was 5.92 MΩ/%RH for entire range RH i.e. 10-90%RH.

The Humidity sensing properties of pellet and film sensor fabricated from B was shown in Figure 2 (b). Figure 2 (b) shows a rapid decrease and fast changes of resistance for a film of B and reveal more sensitivity 25.82 MΩ/%RH in the range 10-35%RH. The average sensitivity calculated for a film of B was 8.12.

The comparative humidity sensing properties of pellet sensors prepared from A and B is shown in Figure 3 (a). The average sensitivity of pellets of A and B were 4.37 MΩ/%RH and 6.61 MΩ/%RH respectively. Figure 3 (b) shows comparative humidity sensing of films fabricated from A and B. The representation of average sensitivities for pellets and film sensors through bar diagram was shown in Figure 4. The average sensitivities of Pellet A, Film A, Pellet B and Film B were 4.37, 5.92, 6.61 and 8.12 MΩ/% RH respectively.

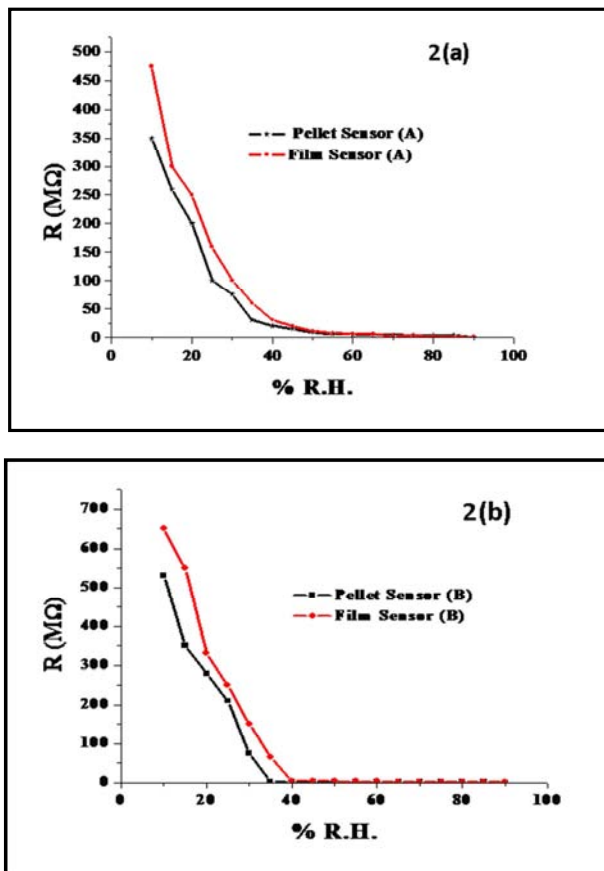


Figure 2. (a) Variations in resistance with %RH for pellet and film prepared using sample A. (b) using sample B.

For all the Pellet/film sensors a decrease in resistance is

observed with increasing humidity levels. At low relative humidity, water adsorption on the sample surface is likely the dominant factor for electronic conduction [35]. Adsorbed water increases the surface electrical conductivity of the ceramic due to the increased charge carrier, protons in the ceramic/water system [36].

The conductivity further increased by the presence of pores on the sample surface. In the first stage of water adsorption, a few water vapor molecules chemisorbs on the grain surfaces by a dissociative mechanism to form two surface hydroxyls per water molecule. In this chemisorbed layer charge transport occurs by the hopping mechanism [37].

With increasing humidity levels, water is physisorbed on top of the chemisorbed layer. Conduction probably occurs by the Grotthus transport mechanism [37]. At these high humidity levels, the layers of physisorbed water molecules tend to condense in capillary pores, with a radius below r_k , the Kelvin radius, given by [38],

$$r_k = \frac{2\gamma M}{\rho RT \ln(P_s / P)}$$

Where P is the water-vapour pressure, P_s is the water vapour pressure at saturation, and γ , ρ and M are the surface tension, density and molecular weight of water, respectively.

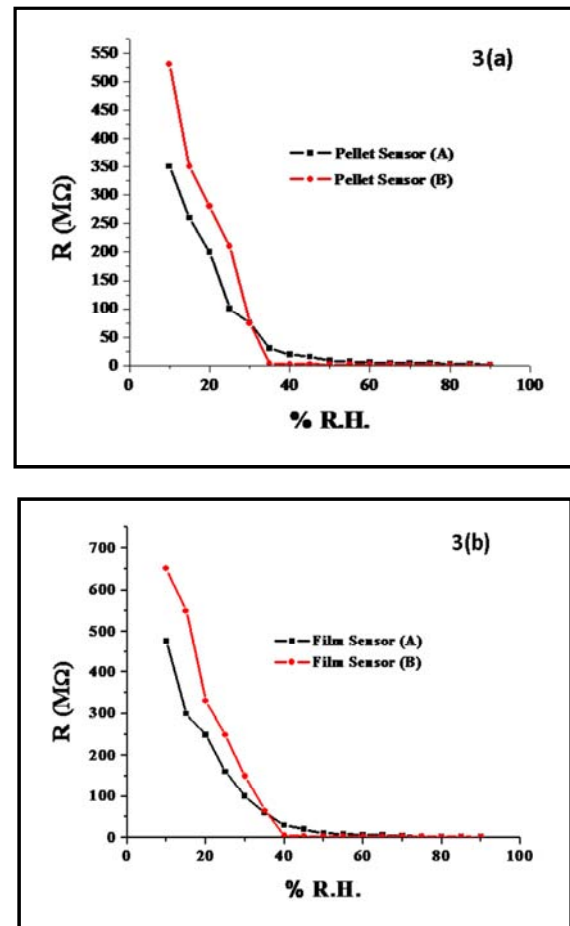


Figure 3. (a) Comparative humidity sensing of pellet sensors prepared using A and B. (b) Comparative humidity sensing of film sensors fabricated using A and B.

An electrolytic conduction in condensed water will take place in addition to the protonic transport in the physisorbed layers [39]. This succession of mechanisms leads to a rapid increase in conduction (decrease in resistance) with increasing humidity content.

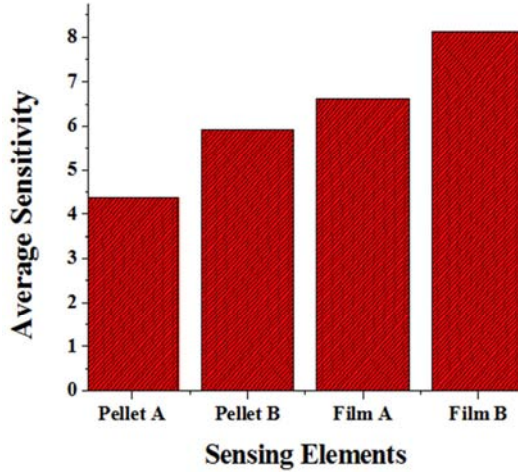


Figure 4. Representation of average sensitivities for pellets and film sensors.

5.2. Hysteresis Measurement

Further experiments have been conducted to determine the hysteresis of the ferrite samples. The humidity chamber was increased from 10-90%RH and then cycled down to 10%RH (indicated in the plots by the dashed line).

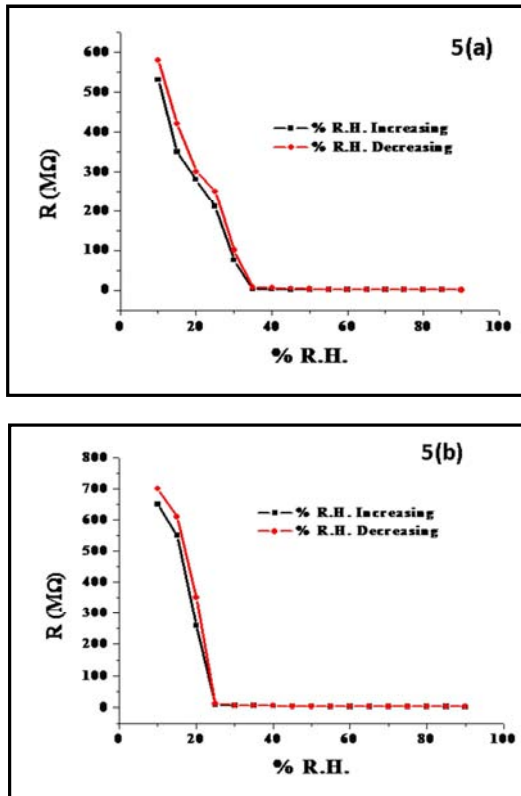


Figure 5. (a) Hysteresis measurement of a thick film fabricated from A (b) Hysteresis measurement of a thick film fabricated from B.

Figure 5 (a) and 5 (b) show measurement of hysteresis for thick films fabricated from A and B. The thick film prepared from material B shows less hysteresis ($\pm 2\%$) as compared to the pellet of B.

5.3. Reproducibility of Humidity Sensing

Results were found to be reproducible after one month. The Film fabricated from material B was most reproducible among all sensors. The reproducibility curve for film sensors of B was shown in Figure 6.

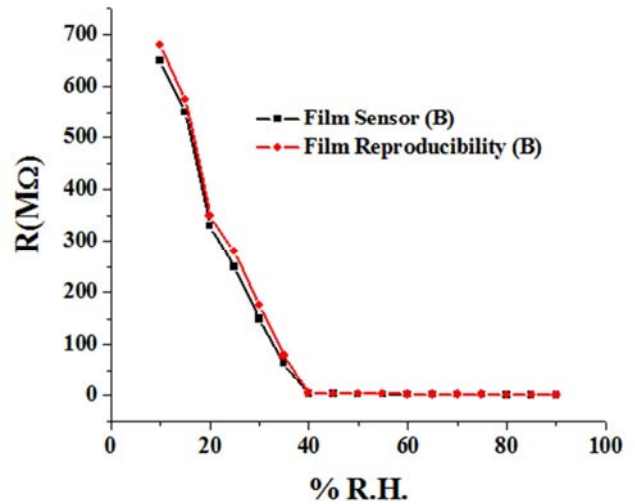
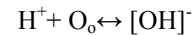


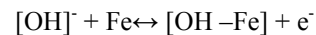
Figure 6. Reproducibility curve of a thick film fabricated using B.

5.4. Humidity Sensing Mechanism of Ferric Oxides

The adsorption of moisture through Ferric oxide surfaces can be understood as follows: The ferrite is porous in nature and has surface oxygen atoms which essentially arise due to the sample preparation technique. When the material adsorbs the humidity, its resistance decreases due to the increase of charge carriers, protons, in the ferrite and water system [40]. The adsorption of water on the surface of the material leads to the dissociation of hydrogen ions. These hydrogen ions bonded with the surface lattice oxygen atom forms the hydroxyl groups [41] as shown in the equation:



Where O_o corresponds to oxygen at lattice sites. The hydroxyl groups thus produced are bonded with the lattice iron atoms and liberate the free electrons [9].



This electron is responsible for electrical conduction. When porous material comes in to contact with the water vapour /moisture, adsorption takes place through different layers and this phenomenon is totally responsible for modulations in conductivity of sensing material. As the sensing material is porous and nanostructured, it provides more free surfaces for adsorption [42].

Thus the experimental results demonstrate that nano-sized

ferric oxide (B) without incorporation of dopants appears to be a promising material for the Humidity sensing.

6. Conclusions

In the present investigation, we have successfully investigated Fe₂O₃ as humidity sensors. The maximum average sensitivities of films prepared as A and B were found 5.92 MΩ/%RH and 8.12 MΩ/%RH respectively. Improved sensing performance of ferric oxide (B) may be attributed to their porous spherical structure and minimum crystallite size as 18 nm. These provide many sites to absorb the water vapor molecule and show the good sensing property. The Fe₂O₃ (sample B) shows maximum sensitivity, less hysteresis, good reproducibility and smaller activation energy at room temperature. These are basic fundamental properties for manufacturing excellent humidity sensor. Thus humidity sensor based on ferric oxide synthesized via hydroxide precipitation is user-friendly, cost effective, easy to fabricate and operable over the entire range of %RH.

References

- [1] R. E. Ruskin, Humidity and Moisture, Reinhold, 1, 1965.
- [2] L. D. Chourp, L. N. Eyrolles, J. F. Okassa, S. C. Fouquenot, M. Souce, H. Marchais, P. Dubois, the Molecular composition of iron oxide nanoparticles, precursors for magnetic drug targeting, as characterized by confocal Raman microspectroscopy, *The Analyst* Vol 130, pp. 1395-1403, 2005.
- [3] P. Brahma, S. Dutta, M. Pal, D. Chakravorty, Magnetic and transport properties of nanostructured ferric oxide produced by mechanical attrition, *J. Appl. Phys.* Vol. 100 pp. 044302-044306, 2006.
- [4] S. S. Nair, M. Mathews, P. A. Joy, S. D. Kulkarni, M. R. Anantharaman, Effect of cobalt doping on the magnetic properties of super paramagnetic γ -Fe₂O₃ polystyrene nanocomposites, *J. Mag. Mag. Mater.* Vol. 283, pp. 344-352, 2008.
- [5] J. Chatterjee, Y. Haik, C. J. Chen, Size-dependent magnetic properties of iron oxide nanoparticles, *J. Mag. Mag. Mater.* Vol. 257, pp.113-118, 2003
- [6] S. Chakrabarti, S. K. Mandal, S. Chaudhuri, Cobalt doped γ -Fe₂O₃ nanoparticles: synthesis and magnetic properties, *Nanotech.* Vol. 16,pp. 506-511, 2005.
- [7] T. N. Narayanan, D. S. Kumar, Y. Yoshida, M. R. Anantharaman, Strain induced anomalous red shift in mesoscopic iron oxide prepared by a novel technique, *Bull. Mater. Sci.* Vol. 31, pp. 759-766, 2008.
- [8] C. L. Zhu, Y. J. Chen, R. X. Wang, L. J. Wang, M. S. Cao, X. L. Shi, Synthesis and enhanced ethanol sensing properties of α -Fe₂O₃/ZnO heterostructures, *Sens. Actuators B: Chem.*, Vol. 140, pp. 185-189, 2009.
- [9] K. Arshaka, K. Twomey, D. Egan, A ceramic Thick Film humidity sensor based on MnZn Ferrite, *Sensors*, Vol. 2, pp. 50-61, 2002.
- [10] A. S. Vaingankar, S. G. Kulkarni, M. S. Sagare, Humidity Sensing using Soft Ferrites, *J. Phy. IV France*, Vol. 7, pp. C1-155-C1-156, 1997.
- [11] C. C. Chai, J. Peng, B. P. Yan, Preparation and gas-sensing properties of α -Fe₂O₃ thin films, *J. Elec. Mat.* Vol 24, pp. 799-804, 1995.
- [12] A. Ray, S. Chakraborty, A. Chowdhury, S. Majumdar, A. Prakash, Ram Pyare, A. Sen, Room temperature synthesis of γ -Fe₂O₃ by sonochemical route and its response towards butane, *Sens. Actuators B: Chem.*, Vol 130, pp. 882-888, 2008.
- [13] N. K. Chaudhari, J. S. Yu, Size control synthesis of uniform β -FeOOH to high coercive field porous magnetic α -Fe₂O₃ nanorods, *J. Phys. Chem.* pp. C 112, 19957-19962, 2008.
- [14] S. Mukherjee, A. K. Pal, EPR Studies on sol-gel derived Fe₂O₃ nanocrystals in SiO₂ matrix, *Proc. Symp. Solid St. Phys.* pp. 205-206, 2003.
- [15] K. M. Reddy, L. Satyanarayana, S. V. Manorama, synthesis of nanocrystalline Ni_{1-x}CO_xMn_xFe_{2-x}O₄: A material for LPG Gas sensing, *Sens. Actuators B: Chem.*, Vol. 89, pp. 62-67, 2003.
- [16] C. V. G. Reddy, S. V. Manorama, V. J. Rao, Preparation and characterization of ferrites as gas sensor materials, *J. Mater. Sci. Lett.* Vol. 19, pp. 775-778, 2000.
- [17] S. L. Darshane, R. G. Deshmukh, S. S. Suryavanshi, I. S. Mulla, Gas-sensing properties of zinc ferrite nanoparticles synthesized by the molten-salt route, *J. Am. Ceram. Soc.* Vol. 91 pp. 2724-2726, 2008.
- [18] R. B. Kamble, V. L. Mathe, Nanocrystalline nickel ferrite thick film as an efficient gas sensor at room temperature, *Sens. Actuators. B* Vol. 131, pp. 205-209, 2008.
- [19] J. Jiang, Y. M. Yang, Facile synthesis of nanocrystalline spinel NiFe₂O₄ via a novel soft chemistry route, *Mater. Lett.* Vol. 61, pp. 4276-4279, 2007.
- [20] E. Rezlescu, N. Iftimie, P. D. Popa, N. Rezlescu, Porous nickel ferrite for semiconducting gas sensor, *J. Phys.* Vol. 15 pp. 51-54, 2005.
- [21] A. A. Bahgatt, M. K. Fayek, A. A. Hamalaway, N. A. Eissaf, The influence of substitution of iron ions on the electron hopping in magnetite, *J. Phys. C: Solid St. Phys.* Vol. 13, pp. 2601-2608, 1980.
- [22] Y. Hotta, S. Ozeki, T. Suzuki, J. Imai, K. Kaneko, *Surface characterization of titanated α -Fe₂O₃*, *Langmuir*, Vol.7, pp. 2649-2653, 1991.
- [23] A. K. Lagashetty, H. Vijayanand, S. Basavaraja, M. D. Bedre, A. Venkataraman, *Preparation, characterization and thermal studies of γ -Fe₂O₃ and CuO dispersed polycarbonatenanocomposites* *J. Therm. Anal. Calorim.* Vol. 99 pp. 577-581, 2010.
- [24] C. Xiangfeng, J. Dongli, Z. Chenmou, *The preparation and gas-sensing properties of NiFe₂O₄ nanocubes and nanorods*, *Sens. Actuators B: Chem.*, Vol. 123. pp. 793-797, 2007.
- [25] Y. J. Chen, C. L. Zhu, L. J. Wang, P. Gao, M. S. Cao, X. L. Shi, Synthesis and enhanced ethanol sensing characteristics of α -Fe₂O₃/SnO₂ core-shell nanorods, *Nanotech.* Vol.20 pp. 1-6, 2009.
- [26] B. S. Kang, H. T. Wang, L. C. Tien, F. Ren, B. P. Gila, D.P. Norton, C. R. Abernathy, J. Lin, S. J. Pearton, Wide band gap semiconductor nano rod and thin film gas sensors, *Sens.* Vol. 6, pp. 643-666, 2006.

- [27] S. Si, C. Li, X. Wang, Q. Peng, Y. Li, Fe₂O₃/ZnO core-shell nanorods for gas sensors, *Sens. Actuators B:Chem.*, Vol. 119 pp. 52-56, 2006.
- [28] B. Shouli, C. Liangyuan, L. Dianqing, Y. Wensheng, Y. Pengcheng, L. Zhiyong, C. Aifan, C.C. Liu, Different morphologies of ZnO nanorods and their sensing property, *Sens. Actuators B: Chem.*, Vol. 146, pp. 129-127, 2010.
- [29] S. Shi, J. Y. Hwang, Microwave-assisted wet chemical synthesis: advantages, significance and steps to industrialization, *J. Min. Mat. Charac. Engg.* Vol. 2 pp. 101-110, 2003.
- [30] J. H. Bang, K.S. Suslick, Sonochemical synthesis of nanosized hollow hematite, *J. Am. Chem. Soc.* 129, pp. 2242-2243, 2007.
- [31] B. C. Yadav, Richa Srivastava, C. D. Dwivedi and P. Pramanik, Moisture sensor based ZnO nanomaterial synthesized through oxalate route, *Sens. Actuators B: Chem.*, Vol. 131, pp. 216-222, 2008.
- [32] B. C. Yadav, Richa Srivastava, Synthesis of nano-sized ZnO using drop wise method and its performances as moisture sensor, *Sensors and Actuators A, Physical*, Vol. 153, pp. 137-141, 2009
- [33] B. C. Yadav, Richa Srivastava and C. D. Dwivedi, Synthesis of ZnO nanomaterials through hydroxide route and their application as Humidity Sensor, *Synthesis and Reactivity in Inorganic, Metal-Organic and Nano - Metal Chemistry*, Vol. 37, pp. 1-7, 2007.
- [34] S. Singh, N. Verma, B. C. Yadav, R. Prakash, A comparative study on surface morphological investigations of ferric oxide for LPG and opto-electronic humidity sensors, *Applied Surface Science*, Vol. 258, pp.8780– 8789, 2012.
- [35] S. C. Kan, K. L. Tzy, L. Feng-Jiin, Sensing mechanism of a porous ceramic as a humidity sensor, *Sens. Actuators B: Chem.*, Vol. 56. 1999, pp. 106-111.
- [36] Richa Srivastava, B. C. Yadav, Monika Singh, T. P. Yadav, "Synthesis, characterization of Nickel Ferrite and its uses as Humidity & LPG sensors," *J. of Inorgani and Organometallic Polymers and Materials*, DOI 10.1007/s10904-016-0425-4, 2016.
- [37] W. M. Sears, The effect of oxygen stoichiometry on the humidity sensing characteristics of bismuth iron molybdate, *Sens. Actuators B: Chem.*, Vol. 67, pp. 161-172, 2000.
- [38] Richa Srivastava, B. C. Yadav, Nanostructured ZnO, ZnO-TiO₂ and ZnO-Nb₂O₅ as solid state humidity sensor, *Advanced Material Letters* Vol. 3, pp. 197-203 2012.
- [39] W. Qu, W. Wlodarski, J. U. Meyer, Comparative study on micromorphology and humidity sensitive properties of thin-film and thick-film humidity sensors based on semiconducting MnWO₄, *Sens. Actuators B:Chem.*, Vol. 64, pp. 76-82 2000.
- [40] X. Q. Liu, S. W. Tao, Y. S. She, Preparation and characterization of nanocrystalline α -Fe₂O₃ by sol-gel process, *Sens. Actuators B: Chem.*, Vol. 40, pp. 161-165, 1997.
- [41] K. Suri, S. Annapoorni, A. K. Sarkar, R. P. Tandon, Gas and humidity sensors based on iron oxide-polypyrrole nanocomposites, *Sens. Actuators B:Chem.*, Vol. 81, pp. 277-282, 2000.
- [42] B. C. Yadav, K. S. Chauhan, S. Singh, R. K. Sonker, S. Sikarwar and R. Kumar, Growth and characterization of sol-gel processed rectangular shaped nanostructured ferric oxide thin film followed by humidity and gas sensing, *J Mater Sci: Mater Electron*, Vol. 28, Issue 7, pp. 5270–5280, 2017.